





## ORIGINAL PAPER

# ETS1 phosphorylation at threonine 38 is associated with the cell of origin of diffuse large B cell lymphoma and sustains the growth of tumour cells

Elaine Y. L. Chung<sup>1</sup> | Giulio Sartori<sup>1</sup> | Maurilio Ponzoni<sup>2</sup>  | Luciano Cascione<sup>1,3</sup> |  
 Valdemar Priebe<sup>1</sup> | Zijun Y. Xu-Monette<sup>4</sup> | Xiaosheng Fang<sup>4</sup>  | Mingzhi Zhang<sup>4</sup> |  
 Carlo Visco<sup>5</sup>  | Alexandar Tzankov<sup>6</sup> | Andrea Rinaldi<sup>1</sup> | Jacopo Sgrignani<sup>7</sup> |  
 Emanuele Zucca<sup>8</sup> | Davide Rossi<sup>1,8</sup> | Andrea Cavalli<sup>7</sup> | Giorgio Inghirami<sup>9</sup> |  
 David W. Scott<sup>10,11</sup> | Ken H. Young<sup>4</sup> | Francesco Bertoni<sup>1,8</sup> 

<sup>1</sup>Institute of Oncology Research, Faculty of Biomedical Sciences, USI, Bellinzona, Switzerland

<sup>2</sup>IRCCS San Raffaele Hospital Scientific Institute, Vita Salute San Raffaele University, Milan, Italy

<sup>3</sup>SIB Swiss Institute of Bioinformatics, Lausanne, Switzerland

<sup>4</sup>Duke University Medical Center, Durham, North Carolina, USA

<sup>5</sup>Section of Hematology, Department of Medicine, University of Verona, Verona, Italy

<sup>6</sup>Pathology, Institute of Medical Genetics and Pathology, University Hospital, Basel, Switzerland

<sup>7</sup>Faculty of Biomedical Sciences, Institute for Research in Biomedicine, USI, Bellinzona, Switzerland

<sup>8</sup>Oncology Institute of Southern Switzerland, Ente Ospedaliero Cantonale, Bellinzona, Switzerland

<sup>9</sup>Pathology and Laboratory Medicine Department, Weill Cornell Medicine, New York, New York, USA

<sup>10</sup>Centre for Lymphoid Cancer, BC Cancer, University of British Columbia, Vancouver, British Columbia, Canada

<sup>11</sup>Department of Medicine, University of British Columbia, Vancouver, British Columbia, Canada

## Correspondence

Francesco Bertoni, Institute of Oncology Research, via Francesco Chiesa 5, Bellinzona 6500, Switzerland.  
 Email: [francesco.bertoni@ior.usi.ch](mailto:francesco.bertoni@ior.usi.ch)

## Funding information

Rotary Foundation, Grant/Award Number: GG1639200 and GG1756935; Swiss Cancer Research Foundation, Grant/Award Number: KLS-3580-02-2015

## Summary

The transcriptional factor ETS1 is upregulated in 25% of diffuse large B cell lymphoma (DLBCL). Here, we studied the role of ETS1 phosphorylation at threonine 38, a marker for ETS1 activation, in DLBCL cellular models and clinical specimens. p-ETS1 was detected in activated B cell-like DLBCL (ABC), not in germinal centre B-cell-like DLBCL (GCB) cell lines and, accordingly, it was more common in ABC than GCB DLBCL diagnostic biopsies. MEK inhibition decreased both baseline and IgM stimulation-induced p-ETS1 levels. Genetic inhibition of phosphorylation of ETS1 at threonine 38 affected the growth and the BCR-mediated transcriptome program in DLBCL cell lines. Our data demonstrate that ETS1 phosphorylation at threonine 38 is important for the growth of DLBCL cells and its pharmacological inhibition could benefit lymphoma patients.

## KEYWORDS

11q24.3 gain, diffuse large B-cell lymphoma (DLBCL), ETS1 Thr38 phosphorylation, MEK/ERK axis

Elaine Y. L. Chung and Giulio Sartori contributed equally to this work.

This is an open access article under the terms of the [Creative Commons Attribution-NonCommercial-NoDerivs](https://creativecommons.org/licenses/by-nc-nd/4.0/) License, which permits use and distribution in any medium, provided the original work is properly cited, the use is non-commercial and no modifications or adaptations are made.

© 2023 The Authors. *British Journal of Haematology* published by British Society for Haematology and John Wiley & Sons Ltd.

## BACKGROUND

Diffuse large B cell lymphoma (DLBCL) is the most common form of aggressive lymphoma, comprising 30%–40% of all newly diagnosed cases.<sup>1</sup> Gene-expression profiling (GEP) identified two main distinct DLBCL subtypes, the activated B cell-like (ABC) and germinal centre B cell-like (GCB) DLBCL, which have been better subdivided into genetically defined subclusters.<sup>1–4</sup> GCB DLBCL has tonic B cell receptor (BCR) signalling and expresses genes found in normal germinal centres, while ABC DLBCL is driven by chronically active BCR signalling,<sup>2</sup> which leads to constitutive stimulation of the nuclear factor  $\kappa$ B (NF- $\kappa$ B) pathway. ABC DLBCL patients display inferior outcomes following standard R-CHOP treatment but a better response to novel agents (ibrutinib or lenalidomide) than patients with GCB DLBCL.<sup>1</sup> We previously identified a recurrent gain mapping to chromosome 11q24.3 in 23% of 166 analysed DLBCL cases, and the transcription factors ETS1 and FLI1, located within the 11q24.3 region, have higher expression in clinical samples carrying the gain.<sup>5</sup> These two transcription factors largely co-regulate a series of genes involved in B cell signalling, differentiation and cell cycle.<sup>5–7</sup> FLI1 is expressed at a higher level in GCB than ABC DLBCL,<sup>7</sup> while ETS1 levels are higher in ABC than GCB DLBCL.<sup>5,6</sup>

ETS factors family shares a unique DNA binding domain called the ‘ETS’ domain; in addition, several ETS proteins, including ETS1 and FLI1, contain a conserved region known as the ‘Pointed’ domain that is involved in protein–protein interactions. In ETS1, the Pointed domain serves as a docking site for extracellular regulated kinases (ERKs), which subsequently phosphorylate the protein at threonine (Thr) 38 located upstream of the Pointed domain.<sup>8</sup> The phosphorylation of this conserved residue leads to enhanced transcriptional activity of ETS1<sup>9</sup> by promoting the recruitment of co-activators such as p300/CREB binding protein (CBP).<sup>10,11</sup> These findings underscore the functional role of Thr38 phosphorylation in ETS1 transcriptional activity. Here, we studied the pathogenetic role of this specific ETS1 phosphorylation in DLBCL.

## METHODS

### Immunohistochemistry

Immunohistochemistry was performed on formalin-fixed, paraffin-embedded sections from three cohorts of cases, two derived from the International DLBCL Rituximab-CHOP Consortium Program Study<sup>12</sup> ( $n=14$  and  $n=315$ ) and one from the BC Cancer Agency (BCCA) Lymphoid Cancer<sup>13</sup> ( $n=230$ ). Following a deparaffinization/rehydration step and washing slides in serial baths with Xylene 100%, EtOH (100%–95%–80%–70%) and H<sub>2</sub>O MilliQ, immunostaining with anti-phospho-ETS1 (Thr38; no. 59179, Abcam) was performed with an automated immunostainer (Benchmark XT, Ventana Medical Systems) after heat-induced epitope retrieval, which was carried out using

Ventana cell conditioning buffer 1 (CC1) for 60 min. Cases were scored as positive whenever more than 10% of neoplastic cells were immunoreactive for the marker. All patients provided informed consent in accordance with the hospital's institutional review board and the Declaration of Helsinki.

### Cell lines

A total of 19 human established cell lines were used: 11 from GCB DLBCL (SU-DHL-4, Farage, DoHH2, Karpas-422, OCI-LY-1, OCI-LY-8, SU-DHL-6, VAL, OCI-LY-7, Pfeiffer and Toledo) and seven from ABC DLBCL (RCK-8, RIVA, HBL-1, OCI-LY-3, OCI-LY-10, SU-DHL-2, TMD8 and U2932) (Table S1). All culture media were supplemented with foetal bovine serum (10%), penicillin–streptomycin–neomycin (approximately 5000 units penicillin, 5 mg streptomycin and 10 mg neomycin/mL, Sigma) and L-glutamine (1%). Cell line identity was confirmed by short tandem repeat (STR) DNA profiling, as previously described.<sup>14</sup> All experiments were performed within 1 month from thawing, and the cells were regularly tested to be free from Mycoplasma contamination using MycoAlert (Lonza).

### Immunoblotting

Protein extraction, separation and immunoblotting were performed as previously described.<sup>7</sup> Anti-IRF4 (no. 4964, Cell Signaling Technology), anti-ERK (sc-93, Santa Cruz Biotechnology), anti-phospho-ERK (tyr204; sc-7383, Santa Cruz Biotechnology), anti-ETS1 (sc-350, Santa Cruz Biotechnology), anti-phospho-ETS1 (Thr38; no. 59179, Abcam), anti-HA (no. A01244, GenScript) and anti-GAPDH (no. 100242, Sino Biologicals) antibodies were used for immunoblotting. For rescue experiments, lysates were run on 15-well precast 4–20% gradient gel (no. 4561096, BioRad).

### BCR stimulation and drugs treatment

U2932 and TMD8 cells were seeded at  $1 \times 10^6/2$  mL/well in a 6-well plate and were cultured either unstimulated or stimulated with 5  $\mu$ g of  $\mu$  chain specific anti-human IgM (no. 2022-01, Southern Biotech) for 20', followed by treatment with either solvent, dimethyl sulphoxide (DMSO) or 0.5  $\mu$ M pimasertib (Selleckchem), for 30' or 2 h prior to harvest.

### Molecular dynamics simulation

Molecular dynamics simulations were performed starting from the structure of Ets-1 PNT domain (PDB ID code 2JV3). The T38V mutation was prepared using the Maestro graphic interface. The protonation state of protein histidine residues at pH 7 was assigned using Propka.<sup>15</sup> The protein structures were then solvated in box of water with minimal

distance from the protein surface of 10 Å. The neutrality of the system was ensured by adding the proper number of counter ions. All the non-solvent molecules were described by the OPLS3<sup>16</sup> force field, while TIP3P model<sup>17</sup> was used for water molecules. The pressure and the temperature were fixed at 300 K and 1 atm by the Martyna-Tobias-Klein NPT thermostat scheme. The entire systems were simulated for 1 μs and the secondary structure of the protein over the trajectory was analysed by VMD software.<sup>18</sup>

## Viral transduction

HEK293T cells were seeded in 10 cm<sup>2</sup> dishes at 2 × 10<sup>6</sup> density, cultured in 10 mL of 1 × DMEM +4.5 g/L D-glucose (no. 61965-059, Invitrogen) supplemented with 10% FBS 1% penicillin/streptomycin/dish. Cells were transfected with viral plasmids along with third-generation packaging vectors using jetPRIME reagents (no. 114-07, Polyplus Transfection) according to the manufacturer's instructions. Medium was replaced with culture medium for either U2932 or Karpas-422 16 h post-transfection. Three infections were performed 48 h after the medium change, with the first, second and third infection spanning 5, 16 and 5 h respectively. Viral supernatants were filtered through 0.45 μm filters followed by supplementation with polybrene (4 μg/μL) at 1–500 dilution. Infection occurred at a ratio of 0.5 × 10<sup>6</sup> target cells/3 mL of viral supernatant. U2932 and Karpas-422 cells were first infected with either wild-type (WT) or Thr38Val mutant (MUT) ETS1 HA\_pMx-ires-GFP. Cells were sorted to enrich for >90% GFP positivity prior to secondary infection with ETS1-specific shRNA, pRS19-U6-(shETS1)-UbiC-TagRFP-2A-Puro. Flow cytometry was used to assess infection efficiency according to the percentage of GFP and RFP double-positive U2932 and Karpas-422 cells; transduced cells were maintained in 1 and 0.8 μg of puromycin/ml of culture medium, respectively.

## Proliferation assay

Proliferation of transduced cells in vitro was determined using cell proliferation reagent WST-1 (no. 11644807001, Roche). Cells were seeded at 4 × 10<sup>3</sup> cells per well in triplicates with 100 μL culture medium/well in a 96-well plate. Proliferation status was determined every 24 h by incubating with 10 μL of cell proliferation reagent WST-1 for 4 h. Absorbance of the treated samples was measured against blank control (medium alone) at 450 nm using Cytation 5 microplate reader.

## Statistical analysis

The data are presented as mean ± standard deviation (SD) of three or more independent results unless otherwise noted. A two-tailed Student's *t*-test was performed to determine the statistical significance. Categorical variables were compared

by  $\chi^2$  test and Fisher's exact test when appropriate. *p* value <0.05 was considered significant.

## RNA-Seq

Samples were obtained from U2932 cells transduced with either WT or MUT ETS1 HA\_pMx-ires-GFP and pRS19-U6-(shETS1)-UbiC-TagRFP-2A-Puro. Cells were either unstimulated or stimulated with  $\mu$  chain-specific IgM for 1 h prior to RNA harvest. Three independent biological experiments were performed. Initial RNA quality control was performed on the Agilent BioAnalyzer (Agilent Technologies) using the RNA 6000 Nano kit (Agilent Technologies) and concentration was determined with the Invitrogen Qubit (Thermo Fisher Scientific) using RNA BR reagents (Thermo Fisher Scientific). Total RNA samples were prepared for RNA-Seq with the NEBNext rRNA Depletion kit, the NEBNext Ultra Directional RNA Library Prep Kit for Illumina and NEBNext Multiplex Oligos for Illumina (New England BioLabs Inc.). Sequencing was performed using a NextSeq 500 with the NextSeq 500/550 High Output Kit v2 (150 cycles PE; Illumina).

## Data-mining

All bioinformatic processing was performed using R/Bioconductor software packages in RStudio. RNA-Seq raw reads were quality assessed using fastqc.<sup>19</sup> For each sample the distribution of unique, multi- and unmapped reads were checked for a high proportion of unmapped or multi-mapped reads. Reads obtained from RNA sequencing were mapped against the human hg38 genome build using the Genecode version 22 annotation.<sup>20</sup> Alignment was done with STAR (v2.4.0h)<sup>21</sup> and counting of reads overlapping gene features with HTSeq-Count.<sup>22</sup> Transcripts with a count-per-million greater than one in at least three samples underwent differential gene expression analysis was performed using the voom/limma<sup>23</sup> R package. Functional annotation was performed with *g:Profiler* on transcripts bearing a *p* < 0.05, using gene sets from the Molecular Signatures Database (MSigDB v5.1)<sup>24</sup> (Hallmark, c2.all, c5.bp, c6), SignatureDB<sup>25</sup> and from different publications as indicated, using *default analysis settings for g:Profiler*.<sup>26</sup> Heatmaps of normalized expression values (log<sub>2</sub> CPM) of the genes modulated (*p* < 0.05) and belonging to specific genesets were plotted using edgeR,<sup>27</sup> limma<sup>23</sup> and made4<sup>28</sup> with alphabetical sorting of columns and rows based on the log<sub>2</sub> fold-change of the comparison of interest.

Publicly available gene-expression profiling (GEP) data from clinical specimens, produced using the HG-U133 Plus 2.0 GeneChips (Affymetrix), was retrieved from the GSE31312 dataset.<sup>29</sup>

Differential gene expression analysis was performed using the voom/limma<sup>23</sup> R package, followed by functional annotation with preranked GSEA (Gene Set Enrichment Analysis) on fold change-ranked values, using the same gene sets collection as for RNA-Seq.

## RESULTS

### ETS1 is phosphorylated at threonine 38 in diffuse large B cell lymphomas

ETS1 expression is upregulated in DLBCL bearing the chromosomal gain at 11q24.3.<sup>5</sup> We assessed the phosphorylation of the conserved threonine 38 residue, known to enhance the transactivation activity of ETS1,<sup>9,10</sup> in DLBCL cases with 11q gain. Nuclear expression of p-ETS1-Thr38 was seen in four out of four DLBCL clinical specimens (Figure 1) previously reported to overexpress ETS1 due to the 11q gain.<sup>5</sup>

Subsequently, we evaluated p-ETS1-Thr38 levels in a panel of 19 DLBCL cell lines (Figure 2A). All cell lines expressed total ETS1. We found that p-ETS1 was detected in all (8/8) ABC DLBCL cell lines, with high expression in most of them, and only in 18.2% (2/11) of GCB DLBCL cell lines (Pfeiffer and Toledo) (100% vs. 18.2% p-ETS1-Thr38+,  $p=0.0024$ ). Interferon Regulatory Factor 4 (IRF4), also known as MUM1, a key transcription factor in B cell differentiation and activation,<sup>30</sup> is a marker for ABC DLBCL<sup>31</sup> and ERK has been known as the upstream kinase of ETS1 in other cellular systems.<sup>9,10,32</sup> Hence, we studied the protein expression of IRF4 and of the total and phosphorylated forms of ERK. IRF4 was expressed in all 8/8 ABC DLBCL (100%) and 0/11 GCB cell lines (0%). While all 19 cell lines expressed total ERK, p-ERK-Tyr204 was detectable in 6/8 ABC (75%) and 2/11 GCB (18.2%) (75% vs. 18.2% p-ERK-Tyr204+,  $p=0.037$ ), very similarly to p-ETS1.

Based on these data, since ETS1 is a transcription factor and p-ETS1-Thr38 is a marker for its activation, we investigated the expression patterns with the nucleus and

cytoplasm distribution in five ABC DLBCL cell lines. The presence of total ETS1 and especially of p-ETS1-Thr38 was predominantly in the nucleus of all cell lines (Figure 2B).

### B cell receptor signalling mediates ETS1 phosphorylation at threonine 38

To understand the mechanisms sustaining the presence of p-ETS1-Thr38 in ABC DLBCL, we stimulated BCR signalling with anti-IgM in two ABC DLBCL cell lines (U2932 and TMD8) expressing relatively low p-ETS1-Thr38 levels compared to other ABC DLBCL cell lines. BCR stimulation led to an increase in p-ETS1-Thr38 and p-ERK-Tyr204 in both cell lines, although with different kinetics in the two cell lines (Figure 2C). Conversely, the pharmacological inhibition of MEK, an upstream kinase of ERK, with pimasertib decreased the baseline levels of p-ETS1-Thr38 and counteracted the upregulation of Thr38 induced by IgM stimulation (Figure 2C). These data demonstrate that ETS1 phosphorylation at Thr38 is downstream of MEK/ERK in DLBCL cells.

### Absence of ETS1 phosphorylation at threonine 38 impairs growth of both GCB and ABC DLBCL cell lines

To understand the function of p-ETS1-Thr38 in DLBCL, we created two ETS1 constructs, one wild type (WT) and one with a Thr38Val mutation ETS1 (MUT). The Thr38Val mutation cannot be phosphorylated due to the replacement of the hydroxyl group in the threonine with a methyl substituent

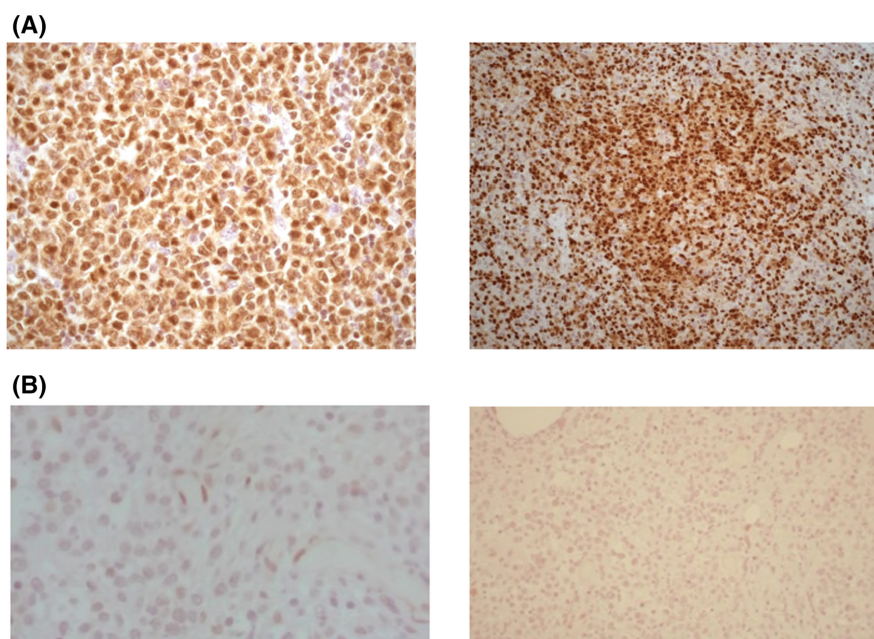


**FIGURE 1** ETS1 Thr38 phosphorylation is detected in DLBCL clinical specimens bearing chromosome 11q24.3 gain. (A) Immunohistochemistry staining showing ETS1 Thr38 phosphorylation in two representative DLBCL clinical specimen bearing 11q gain. (B) Two DLBCL clinical samples with no ETS1 Thr38 phosphorylation at immunohistochemistry.

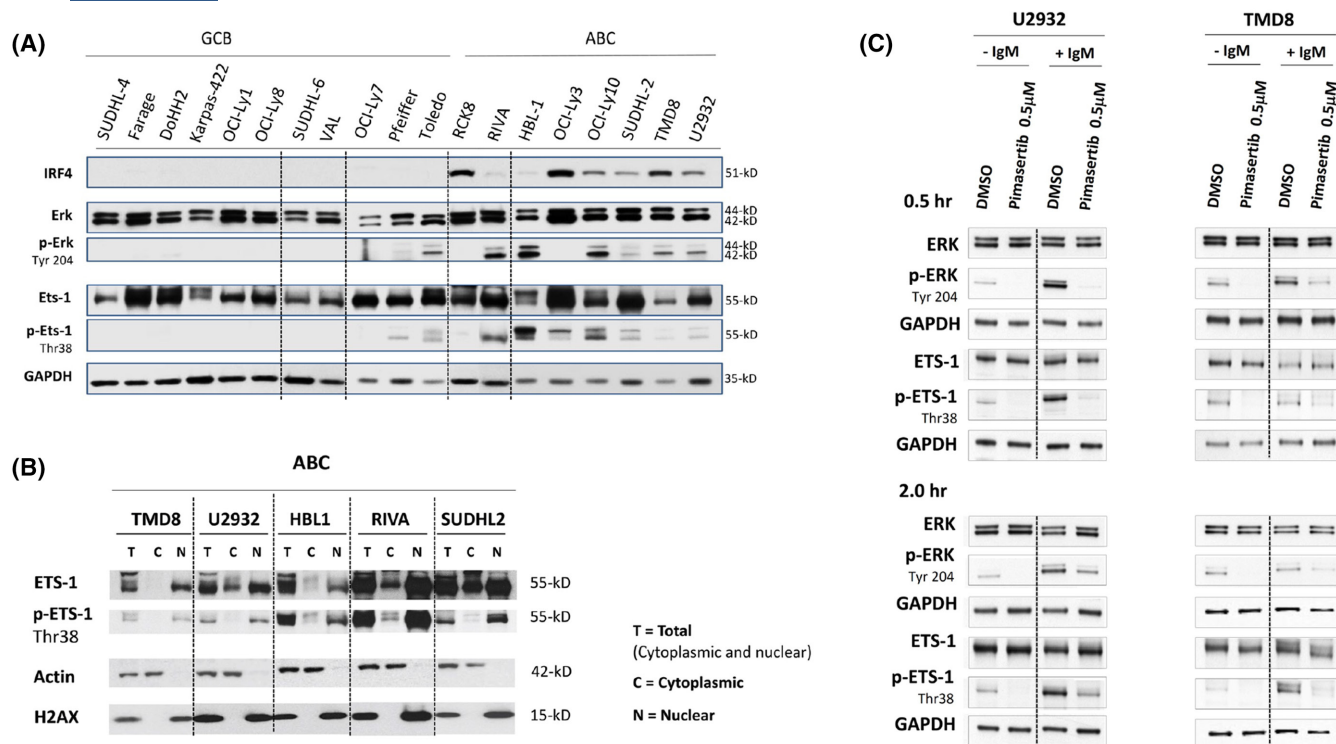


**FIGURE 2** ETS1 Thr38 Phosphorylation is more common in ABC than in GCB DLBCL cell lines and downstream to B cell receptor signalling and MEK. (A) ETS1 and ERK1 are phosphorylated in the majority of ABC DLBCL cell lines. Protein lysates harvested from GCB and ABC DLBCL cell lines were immunoblotted for IRF4, ERK (total and p-Tyr204), and ETS1 (total and p-Thr38) with GAPDH serving as loading control. (B) Nuclear localization of ETS1 (total and p-Thr38); Actin and H2AX were used as markers for cytoplasm and nucleus respectively. (C) p-ETS1-Thr38 is effectively inhibited by the MEK inhibitor pimasertib in two ABC DLBCL cell lines. U2932 and TMD8 cells were either unstimulated or stimulated with anti-IgM for 20 min followed by treatment with pimasertib (500 nM), or DMSO as solvent control in the absence or presence of anti-IgM. Protein lysates were harvested at 0.5 and 2 h postdrug treatment.

in the valine, although it does not impact the normal protein folding as verified by molecular dynamics simulation for 1 microsec (Figure S1). Both constructs also contained a silent mutation in the ETS1 shRNA-targeting site, allowing the shRNA-mediated silencing of the endogenous, but not of the exogenous, ETS1 in one ABC (U2932) and one GCB (Karpas-422) DLBCL cell line (Figure 3A; Figure S1). In agreement with previous reports,<sup>5,6</sup> the absence of ETS1 decreased the growth of both GCB and ABC DLBCL cell lines (Figure 3B). The growth impairment due to endogenous ETS1 knockdown was restored by ETS1 WT but not by Thr38Val construct (Figure 3B). These results underlined the contribution of ETS1 phosphorylation at threonine 38 to the growth of both GCB and ABC DLBCL cell lines.

Next, a transcriptome analysis was performed in wild type and Thr38Val mutant *ETS1* U2932 after knockdown of endogenous ETS1, with and without IgM stimulation (Table S2). Genes involved in signalling regulated by NF-κB, IL2/STAT5 and mTORC1 and downregulated by ibrutinib were enriched among the transcripts upregulated after IgM stimulation in WT U2932. A similar pattern was observed for ETS1 targets (Figure 3C; Figure S2 and Table S2). IgM stimulation in mutant cells led to similar changes seen in WT cells, but without the upregulation of ETS1 targets, which were not affected in the cells lacking the phosphorylation at Thr38 (Figure 3C; Table S2). Collectively, these results

showed that, in DLBCL, phosphorylation at Thr38 is fundamental for the transcriptional activity of ETS1 and that part of the transcriptional changes induced by IgM stimulation are mediated by this transcription factor.

### ETS1 phosphorylation at threonine 38 is associated with ABC DLBCL in clinical specimens

Since our cell lines data indicated an association between p-ETS1-Thr38 and the ABC DLBCL phenotype, we assessed p-ETS1-Thr38 by immunohistochemistry on DLBCL clinical specimens. In a small, earlier series of 14 DLBCL cases classified for cell of origin using the Hans algorithm, the percentage of p-ETS1-Thr38 positive cells was higher in non-GCB (5/7) than in GCB DLBCL cases (2/7) ( $p = 0.023$ ; Table S3), in agreement with the cell line data. Positive cases most frequently displayed nuclear p-ETS1-Thr38 (Table S3).

We then extended the analysis to two additional cohorts of DLBCL. The presence of p-ETS1-Thr38 was confirmed to be more frequent in ABC than in GCB cases [79% (123/155) vs. 57% (91/160) ( $p < 0.001$ )] among the 315 GEP-classified de novo DLBCL cases from the International DLBCL Rituximab-CHOP Consortium Program Study<sup>12</sup>

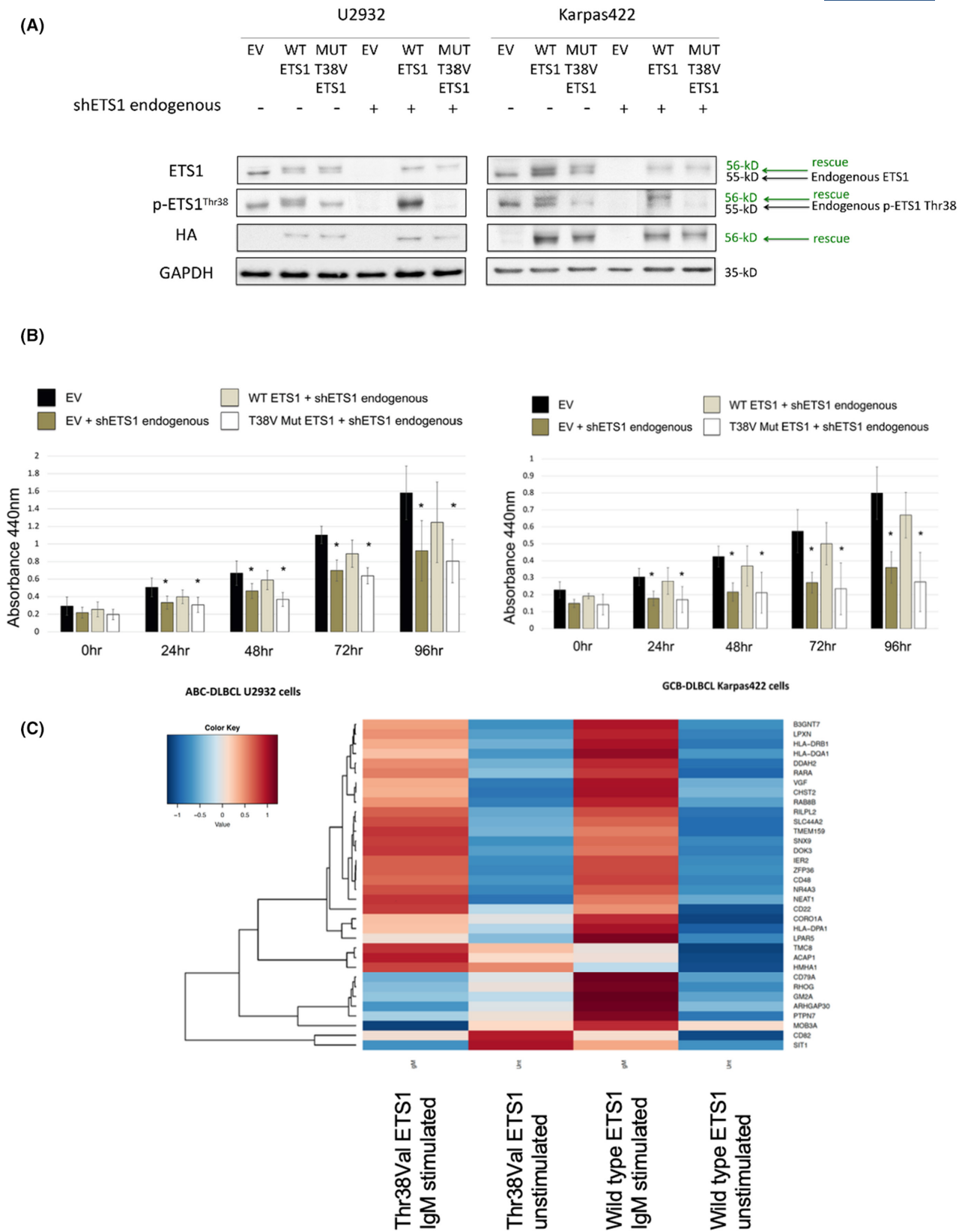


**FIGURE 3** Mutation at p-ETS1-T38V impedes growth in both ABC and GCB DLBCL cells. (A) Immunoblot performed on protein lysates harvested from ABC DLBCL U2932 cells and GCB DLBCL Karpas422 cells expressing exogenous ETS1 constructs with and without knockdown of endogenous ETS1. (B) WST growth assay performed in ABC DLBCL U2932 cells and GCB DLBCL Karpas422 cells expressing exogenous ETS1 constructs with and without knockdown of endogenous ETS1 over the time course from 0 to 96h. Experiments were performed in four biological replicates. \**p*-value  $\leq 0.05$ . (C) Heatmap of ETS1 targets regulated in wild type and not in Thr38Val mutant ETS1 U2932 after knockdown of endogenous ETS1, with and without IgM stimulation.

(Figure 4A). These findings were not confirmed in 230 GEP-classified de novo DLBCL cases from the BC Cancer Agency (BCCA) Lymphoid Cancer<sup>13</sup> (Figure S3).

The presence of p-ETS1 was associated with inferior progression free survival (PFS) at univariate analysis ( $p=0.034$ ) in the GCB-DLBCL of the International DLBCL Rituximab-CHOP Consortium Program Study (Figure 4B). The prognostic impact was also maintained in a multivariate analysis including the International Prognostic Index (IPI) (Table S4). No effect on the outcome was seen in ABC DLBCL (Figure 4C).

## ETS1 phosphorylation at threonine 38 is associated with oncogenic signatures

ETS1 Thr38 phosphorylation was associated with high proliferation gene expression signatures in both GCB ( $n=91$ ) and ABC ( $n=123$ ) clinical specimens compared to p-ETS1 negative GCB ( $n=69$ ) or ABC ( $n=32$ ) DLBCL. Genes involved in mitotic spindle, signalling regulated by mTORC1, E2F and G2M, together with MYC targets and genes downregulated by dasatinib were enriched among the transcripts upregulated in p-ETS1 positive

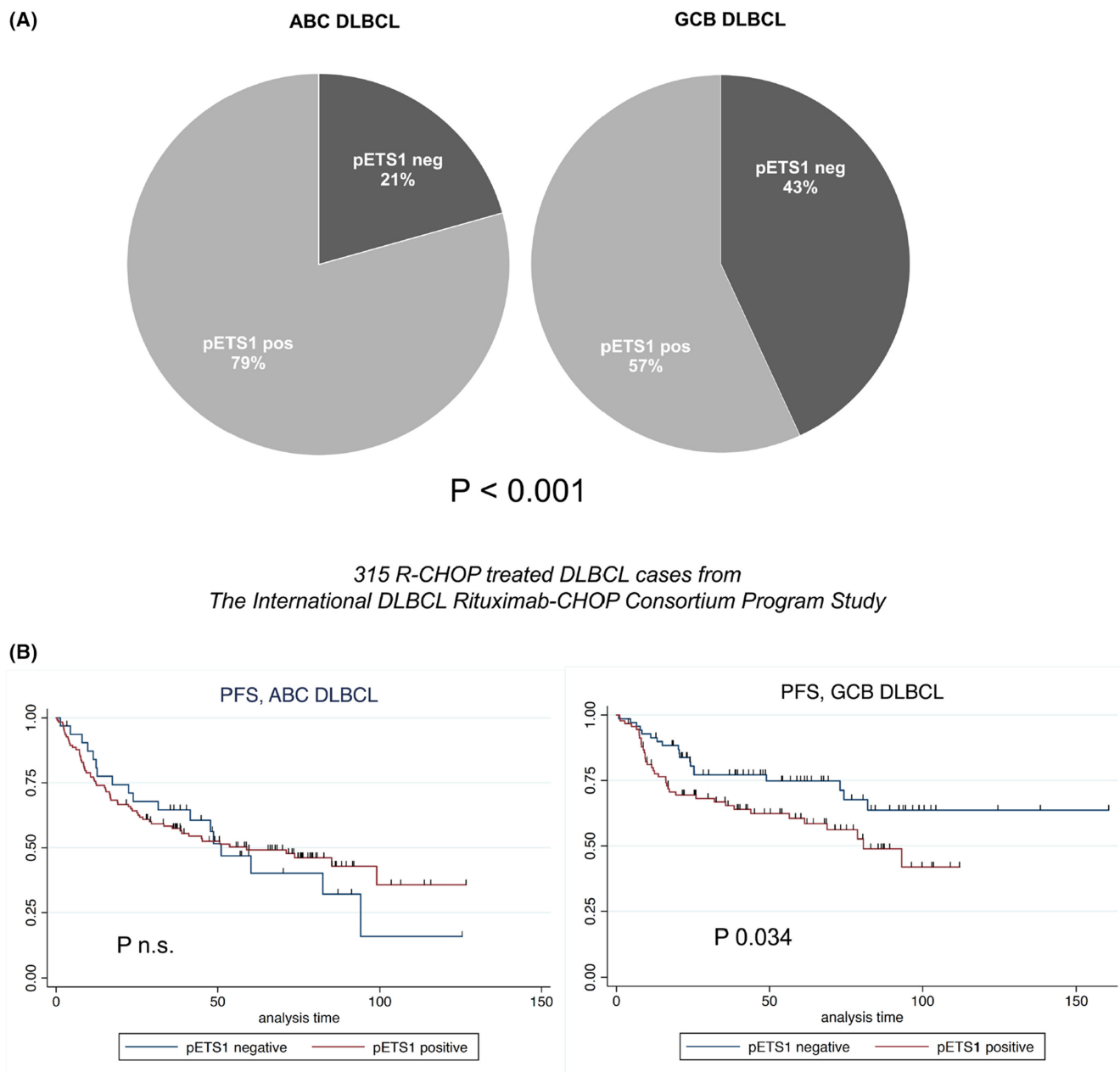


**FIGURE 4** p-ETS1 is more common in ABC DLBCL tumours but is associated with inferior outcomes in GCB DLBCL cases, provided by The International DLBCL Rituximab-CHOP Consortium Program Study. (A) Percentage of p-ETS1 positive cases in GEP classified DLBCL cases. (B) Progression Free Survival (PFS) Kaplan–Meier curve, based on ETS1 Thr38 phosphorylation status, of 160 R-CHOP treated GCB and (C) 155 R-CHOP treated ABC DLBCL patients (X-axis, months; Y-axis, percentage of patients free of progression).

samples (Table S5). Statistically significant gene expression enrichment of hallmark signatures, related to cell cycle, were also confirmed by GSEA analysis: E2F targets (NES 1.91 FDR <0.001 in ABC and NES 1.75 FDR 0.002 in GCB), mTORC1 signalling (NES 1.74 FDR 0.006 in ABC and NES 1.49 FDR 0.037 in GCB), mitotic spindle (NES 1.82 FDR 0.003 in ABC and NES 1.77 FDR 0.005 in GCB), G2M checkpoint (NES 1.75 FDR 0.005 in ABC and NES 1.61 FDR 0.060 in GCB) and MYC targets (NES 1.64 FDR 0.041 in ABC and NES 1.53 FDR 0.190 in GCB; Figure 5).

## DISCUSSION

Herein, our data indicate that the BCR-mediated ETS1 phosphorylation at threonine 38 is associated with the ABC DLBCL phenotype and may predict inferior outcomes among GCB DLBCL. In addition, we provide evidence that p-ETS1-Thr38 also sustains DLBCL cell growth and that the phosphorylation of ETS1 can be blocked with drugs targeting the MEK/ERK axis.

We demonstrate ETS1 Thr38 phosphorylation by immunohistochemistry on diagnostic specimens of patients with DLBCL carrying genomic gain on chromosome 11q24.3. Immunoblotting of a panel of DLBCL cell lines showed that p-ETS1-Thr38, along with p-ERK expression, is readily detected in ABC DLBCL compared to GCB DLBCL cells. Since ETS1 is a transcription factor and p-ETS1 is marker for its activation, we defined its subcellular pattern of expression (i.e. nuclear and/or cytoplasmic) in some ABC DLBCL cell lines. According to the functionality, p-ETS1 was present predominantly in the nucleus of all cell lines, while total ETS1 was in both cytoplasm and nucleus.

To evaluate the mechanisms sustaining phosphorylation of ETS1, two ABC DLBCL cell lines (U2932 and TMD8) were exposed to the MEK inhibitor pimavertin after or without stimulation with anti-IgM. The inhibition of MEK abolished the increase in p-ETS1 induced by IgM engagement. Similar changes were seen for p-ERK. These findings confirmed that MEK-ERK signalling regulates p-ETS1-Thr38 in DLBCL.

ETS1 was important for growth in both ABC DLBCL and GCB DLBCL, as confirmed by hampered growth with shRNA-mediated knockdown of ETS1 in U2932 and Karpas-422. To elucidate the functional significance of p-ETS1-Thr38 in DLBCL, we knocked down endogenous ETS1 in both cell lines, followed by ectopic expression of shRNA resistant wild type (WT) or Thr38Val mutant (MUT) ETS constructs. Our results demonstrate that the growth mechanism attributed to ETS1 is mediated by Thr38 phosphorylation in both types of DLBCL. Moreover, transcriptome analysis showed that, differently from WT ETS1 cells, Thr38Val mutant ETS1 cells were not able to upregulate the ETS1 targets.

To understand the clinical implications of our findings, we assessed p-ETS1 expression in clinical DLBCL biopsies. The presence of p-ETS1 was confirmed to be more frequent in ABC than in GCB cases in two of three series of DLBCL

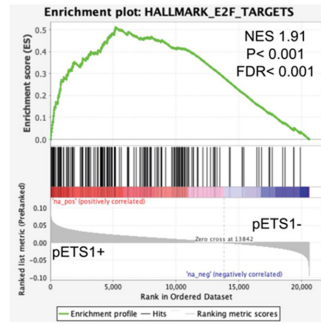
cases. In the large series of 315 de novo DLBCL cases treated with R-CHOP regimen collected by the International DLBCL Rituximab-CHOP Consortium Program Study,<sup>12</sup> unexpectedly, only the p-ETS1 positive GCB DLBCL presented a shorter PFS when compared with p-ETS1 negative cases, while no association with outcome was detected in ABC DLBCL, although the p-ETS1-Thr38 was associated with signatures for high cell cycle-related gene expression in both ABC and GCB DLBCL patients in agreement with the observed effect on cell growth in DLBCL cell lines. This observation might be explained by the balance among different transcription factors, including ETS1 and FLI1, in the various DLBCL subtypes. Focusing on ETS1 and FLI1, despite being both expressed, the two genes show different patterns of expression in GC B cells<sup>33</sup> and in DLBCL subtypes, in which they regulate important shared genes and orchestrate different pathways based on the COO.<sup>5-7</sup> Here, we showed a higher ETS1 phosphorylation in ABC DLBCL, but also that it is present in a subset of GCB DLBCL, in which the transcription factor would act in a different cellular context. Based on recent DLBCL classifications, ETS1 somatic mutations are found mainly in the BN2 genetic subtype (comprising both GCB and ABC DLBCL but enriched for unclassified tumours).<sup>4</sup> In the BN2 cluster, constitutive BCR signalling is confirmed by knockdown of IgM or CD79A, which does not decrease phosphorylation of LYN, SYK, and BTK.<sup>34</sup> Furthermore, ETS1 somatic mutations are associated with significantly shorter survival.<sup>35</sup> More in general, in B cells ETS1 can activate the I $\mu$  heavy chain enhancer<sup>36-39</sup> and lead to PAX5 up-regulation,<sup>40</sup> in this way negatively regulating plasmacytic differentiation. In several cancer types there, is a significant higher or exclusive ETS1 expression when compared to normal tissues as a demonstration of a direct involvement in tumorigenesis and/or drug resistance.<sup>41-45</sup> Interfering with ETS1 phosphorylation could be worth of being investigated in DLBCL as well in other tumours.

In conclusion, with our study, we provide further evidence of the biological and clinical relevance of BCR-mediated ETS1 phosphorylation in DLBCL lymphoma.

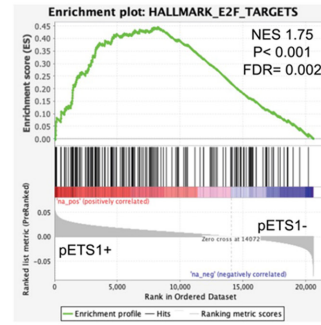
## AUTHOR CONTRIBUTIONS

**Elaine Y. L. Chung, Giulio Sartori:** acquisition, analysis and interpretation of data, drafted the work. **Maurilio Ponzone, David W. Scott, Ken H. Young:** acquisition and analysis of data (collected and characterized tumour samples), provided oversight and helpful advice for the study. **Luciano Cascione:** data mining. **Valdemar Priebe, Zijun Y. Xu-Monette, Xiaosheng Fang, Mingzhi Zhang:** acquisition and analysis of data. **Carlo Visco, Alexandar Tzankov, Giorgio Inghirami:** acquisition and analysis of data (collected and characterized tumour samples). **Andrea Rinaldi:** acquisition of data. **Jacopo Sgrignani, Andrea Cavalli:** modelling. **Emanuele Zucca, Davide Rossi:** provided oversight and helpful advice for the study. **Francesco Bertoni:** conception and design of the work, drafted the work. All authors reviewed the manuscript.

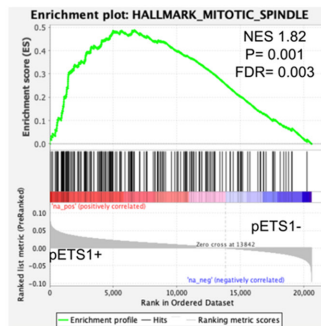




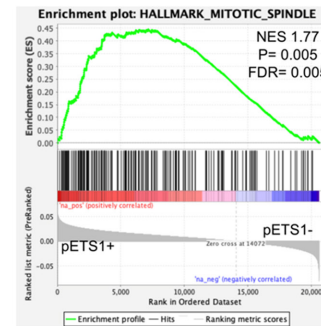
ABC DLBCL



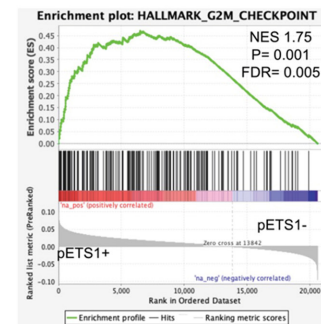
GCB DLBCL



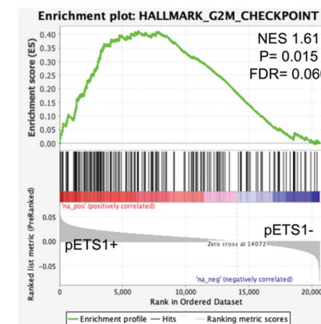
ABC DLBCL



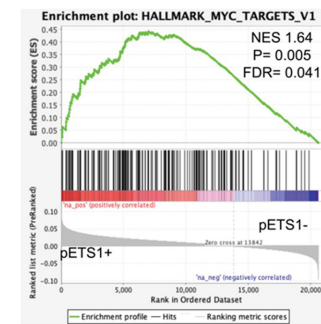
GCB DLBCL



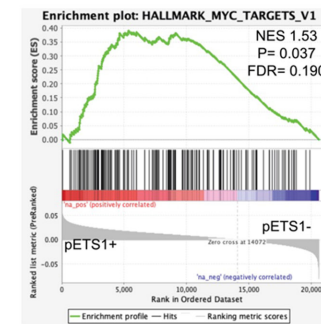
ABC DLBCL



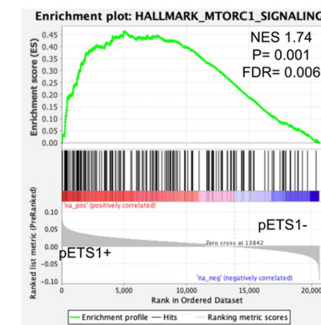
GCB DLBCL



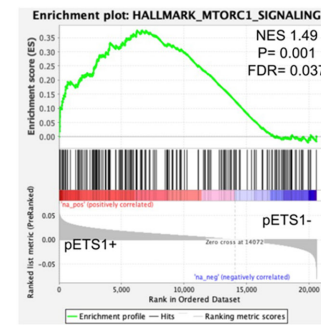
ABC DLBCL



GCB DLBCL



ABC DLBCL



GCB DLBCL

**FIGURE 5** ETS1 phosphorylation at threonine 38 is associated with cell cycle-related and oncogenic signatures. GSEA plots for gene expression signatures were obtained in ABC (left column) and in GCB DLBCL (right column) based on the presence of p-ETS1. Green line, enrichment score; bars in the middle portion of the plots show where the members of the gene set appear in the ranked list of genes; Positive or negative ranking metric indicate respectively correlation or inverse correlation with p-ETS1; FDR, false discovery rate; NES, normalized enrichment score.

## ACKNOWLEDGEMENTS

Open access funding provided by Universita' della Svizzera italiana.

## FUNDING INFORMATION

This work was supported by the Swiss Cancer Research grant KLS-3580-02-2015 (to FB) and by Rotary Foundation grants GG1639200 and GG1756935 (to GS).

## DATA AVAILABILITY STATEMENT

Gene expression data are available at the National Center for Biotechnology Information (NCBI) Gene Expression Omnibus (GEO; <http://www.ncbi.nlm.nih.gov/geo>) database with accession number GSE237548.

## ORCID

Maurilio Ponzoni  <https://orcid.org/0000-0002-0055-325X>

Xiaosheng Fang  <https://orcid.org/0000-0002-4515-9731>

Carlo Visco  <https://orcid.org/0000-0003-2863-0883>

Francesco Bertoni  <https://orcid.org/0000-0001-5637-8983>

## REFERENCES

- Sehn LH, Salles G. Diffuse large B-cell lymphoma. *N Engl J Med*. 2021;384(9):842–58.
- Rosenwald A, Wright G, Chan WC, Connors JM, Campo E, Fisher RI, et al. The use of molecular profiling to predict survival after chemotherapy for diffuse large-B-cell lymphoma. *N Engl J Med*. 2002;346(25):1937–47.
- Chapuy B, Stewart C, Dunford AJ, Kim J, Kamburov A, Redd RA, et al. Molecular subtypes of diffuse large B cell lymphoma are associated with distinct pathogenic mechanisms and outcomes. *Nat Med*. 2018;24(5):679–90.
- Wright GW, Huang DW, Phelan JD, Coulibaly ZA, Roulland S, Young RM, et al. A probabilistic classification tool for genetic subtypes of diffuse large B cell lymphoma with therapeutic implications. *Cancer Cell*. 2020;37(4):551–68. e514.
- Bonetti P, Testoni M, Scandurra M, Ponzoni M, Piva R, Mensah AA, et al. Deregulation of ETS1 and FLI1 contributes to the pathogenesis of diffuse large B-cell lymphoma. *Blood*. 2013;122(13):2233–41.
- Priebe V, Sartori G, Napoli S, Chung EYL, Cascione L, Kwee I, et al. Role of ETS1 in the transcriptional network of diffuse large B cell lymphoma of the activated B cell-like type. *Cancers (Basel)*. 2020;12(7):1912.
- Sartori G, Napoli S, Cascione L, Chung EYL, Priebe V, Arribas AJ, et al. ASB2 is a direct target of FLI1 that sustains NF-kappaB pathway activation in germinal center-derived diffuse large B-cell lymphoma. *J Exp Clin Cancer Res*. 2021;40(1):357.
- Seidel JJ, Graves BJ. An ERK2 docking site in the pointed domain distinguishes a subset of ETS transcription factors. *Genes Dev*. 2002;16(1):127–37.
- Yang BS, Hauser CA, Henkel G, Colman MS, Van Beveren C, Stacey KJ, et al. Ras-mediated phosphorylation of a conserved threonine residue enhances the transactivation activities of c-Ets1 and c-Ets2. *Mol Cell Biol*. 1996;16(2):538–47.
- Foulds CE, Nelson ML, Blaszcak AG, Graves BJ. Ras/mitogen-activated protein kinase signaling activates Ets-1 and Ets-2 by CBP/p300 recruitment. *Mol Cell Biol*. 2004;24(24):10954–64.
- Nelson ML, Kang HS, Lee GM, Blaszcak AG, Lau DK, McIntosh LP, et al. Ras signaling requires dynamic properties of Ets1 for phosphorylation-enhanced binding to coactivator CBP. *Proc Natl Acad Sci U S A*. 2010;107(22):10026–31.
- Xu-Monette ZY, Wu L, Visco C, Tai YC, Tzankov A, Liu WM, et al. Mutational profile and prognostic significance of TP53 in diffuse large B-cell lymphoma patients treated with R-CHOP: report from an International DLBCL Rituximab-CHOP Consortium Program Study. *Blood*. 2012;120(19):3986–96.
- Ennishi D, Mottok A, Ben-Neriah S, Shulha HP, Farinha P, Chan FC, et al. Genetic profiling of MYC and BCL2 in diffuse large B-cell lymphoma determines cell-of-origin-specific clinical impact. *Blood*. 2017;129(20):2760–70.
- Gaudio E, Tarantelli C, Spriano F, Guidetti F, Sartori G, Bordone R, et al. Targeting CD205 with the antibody drug conjugate MEN1309/OBT076 is an active new therapeutic strategy in lymphoma models. *Haematologica*. 2020;105(11):2584–91.
- Olsson MH, Sondergaard CR, Rostkowski M, Jensen JH. PROPKA3: consistent treatment of internal and surface residues in empirical pKa predictions. *J Chem Theory Comput*. 2011;7(2):525–37.
- Harder E, Damm W, Maple J, Wu C, Reboul M, Xiang JY, et al. OPLS3: a force field providing broad coverage of drug-like small molecules and proteins. *J Chem Theory Comput*. 2016;12(1):281–96.
- Jorgensen WL, Chandrasekhar J, Madura JD, Impey RW, Klein LM. Comparison of simple potential functions for simulating liquid water. *J Chem Phys*. 1983;79:926–35.
- Humphrey W, Dalke A, Schulten K. VMD: visual molecular dynamics. *J Mol Graph*. 1996;14(1):33–8.
- Andrews S. FastQC a quality control tool for high throughput sequence data; 2014.
- Harrow J, Frankish A, Gonzalez JM, Tapanari E, Diekhans M, Kokocinski F, et al. GENCODE: the reference human genome annotation for the ENCODE project. *Genome Res*. 2012;22(9):1760–74.
- Dobin A, Davis CA, Schlesinger F, Drenkow J, Zaleski C, Jha S, et al. STAR: ultrafast universal RNA-seq aligner. *Bioinformatics*. 2013;29(1):15–21.
- Anders S, Pyl PT, Huber W. HTSeq—a python framework to work with high-throughput sequencing data. *Bioinformatics*. 2015;31(2):166–9.
- Ritchie ME, Phipson B, Wu D, Hu Y, Law CW, Shi W, et al. Limma powers differential expression analyses for RNA-sequencing and microarray studies. *Nucleic Acids Res*. 2015;43(7):e47.
- Subramanian A, Tamayo P, Mootha VK, Mukherjee S, Ebert BL, Gillette MA, et al. Gene set enrichment analysis: a knowledge-based approach for interpreting genome-wide expression profiles. *Proc Natl Acad Sci U S A*. 2005;102(43):15545–50.
- Shaffer AL, Wright G, Yang L, Powell J, Ngo V, Lamy L, et al. A library of gene expression signatures to illuminate normal and pathological lymphoid biology. *Immunol Rev*. 2006;210:67–85.
- Raudvere U, Kolberg L, Kuzmin I, Arak T, Adler P, Peterson H, et al. g:Profiler: a web server for functional enrichment analysis and conversions of gene lists (2019 update). *Nucleic Acids Res*. 2019;47(W1):W191–8.
- Robinson MD, McCarthy DJ, Smyth GK. edgeR: a Bioconductor package for differential expression analysis of digital gene expression data. *Bioinformatics*. 2010;26(1):139–40.
- Culhane AC, Thioulouse J, Perrière G, Higgins DG. MADE4: an R package for multivariate analysis of gene expression data. *Bioinformatics*. 2005;21(11):2789–90.
- Visco C, Li Y, Xu-Monette ZY, Miranda RN, Green TM, Li Y, et al. Comprehensive gene expression profiling and immunohistochemical studies support application of immunophenotypic algorithm for molecular subtype classification in diffuse large B-cell lymphoma: a

- report from the International DLBCL Rituximab-CHOP Consortium Program Study. *Leukemia*. 2012;26(9):2103–13.
30. Shaffer AL, Emre NC, Romesser PB, Staudt LM. IRF4: immunity. Malignancy! Therapy? *Clin Cancer Res*. 2009;15(9):2954–61.
  31. Blenk S, Engelmann J, Weniger M, Schultz J, Ditttrich M, Rosenwald A, et al. Germinal center B cell-like (GCB) and activated B cell-like (ABC) type of diffuse large B cell lymphoma (DLBCL): analysis of molecular predictors, signatures, cell cycle state and patient survival. *Cancer Inform*. 2007;3:399–420.
  32. Plotnik JP, Budka JA, Ferris MW, Hollenhorst PC. ETS1 is a genome-wide effector of RAS/ERK signaling in epithelial cells. *Nucleic Acids Res*. 2014;42(19):11928–40.
  33. Holmes AB, Corinaldesi C, Shen Q, Kumar R, Compagno N, Wang Z, et al. Single-cell analysis of germinal-center B cells informs on lymphoma cell of origin and outcome. *J Exp Med*. 2020;217(10):e20200483.
  34. Young RM, Phelan JD, Wilson WH, Staudt LM. Pathogenic B-cell receptor signaling in lymphoid malignancies: new insights to improve treatment. *Immunol Rev*. 2019;291(1):190–213.
  35. Pedrosa L, Fernández-Miranda I, Pérez-Callejo D, Quero C, Rodríguez M, Martín-Acosta P, et al. Proposal and validation of a method to classify genetic subtypes of diffuse large B cell lymphoma. *Sci Rep*. 2021;11(1):1886.
  36. Erman B, Sen R. Context dependent transactivation domains activate the immunoglobulin mu heavy chain gene enhancer. *EMBO J*. 1996;15(17):4665–75.
  37. Nelsen B, Tian G, Erman B, Gregoire J, Maki R, Graves B, et al. Regulation of lymphoid-specific immunoglobulin mu heavy chain gene enhancer by ETS-domain proteins. *Science*. 1993;261(5117):82–6.
  38. Rao E, Dang W, Tian G, Sen R. A three-protein-DNA complex on a B cell-specific domain of the immunoglobulin mu heavy chain gene enhancer. *J Biol Chem*. 1997;272(10):6722–32.
  39. Rivera RR, Stuver MH, Steenbergen R, Murre C. Ets proteins: new factors that regulate immunoglobulin heavy-chain gene expression. *Mol Cell Biol*. 1993;13(11):7163–9.
  40. John SA, Clements JL, Russell LM, Garrett-Sinha LA. Ets-1 regulates plasma cell differentiation by interfering with the activity of the transcription factor Blimp-1. *J Biol Chem*. 2008;283(2):951–62.
  41. Lincoln DW 2nd, Bove K. The transcription factor Ets-1 in breast cancer. *Front Biosci*. 2005;10:506–11.
  42. Dittmer J. The biology of the Ets1 proto-oncogene. *Mol Cancer*. 2003;2:29.
  43. Li Y, Wu T, Peng Z, Tian X, Dai Q, Chen M, et al. ETS1 is a prognostic biomarker of triple-negative breast cancer and promotes the triple-negative breast cancer progression through the YAP signaling. *Am J Cancer Res*. 2022;12(11):5074–84.
  44. Luchtel RA, Zhao Y, Aggarwal RK, Pradhan K, Maqbool SB. ETS1 is a novel transcriptional regulator of adult T-cell leukemia/lymphoma of North American descent. *Blood Adv*. 2022;6(20):5613–24.
  45. Huang L, Zhai Y, La J, Lui JW, Moore SPG, Little EC, et al. Targeting pan-ETS factors inhibits melanoma progression. *Cancer Res*. 2021;81(8):2071–85.

## SUPPORTING INFORMATION

Additional supporting information can be found online in the Supporting Information section at the end of this article.

**How to cite this article:** Chung EYL, Sartori G, Ponzoni M, Cascione L, Priebe V, Xu-Monette ZY, et al. ETS1 phosphorylation at threonine 38 is associated with the cell of origin of diffuse large B cell lymphoma and sustains the growth of tumour cells. *Br J Haematol*. 2023;203(2):244–254. <https://doi.org/10.1111/bjh.19018>